

Depletion force between disordered linear macromolecules

Nathaniel Rupprecht, Dervis Can Vural
University of Notre Dame, South Bend, IN
 (Dated: April 27, 2022)

When two macromolecules come very near in a fluid, the molecules that surround them, having finite volume, are less likely to get in between. This leads to a pressure difference manifesting as an entropic attraction, called depletion force. Here we calculate the density profile of liquid molecules surrounding a disordered linear macromolecule, and analytically determine the position dependence of the depletion force between two such molecules. We then verify our formulas with realistic molecular dynamics simulations. Our result can be regarded as an extension of the classical Asakura-Oosawa formula.

Objects immersed or dissolved in a liquid will experience an emergent attractive force, as the liquid molecules, having finite volume, cannot squeeze between them [1]. Put another way, it is entropically favorable for the objects to be close, since each has surrounding volumes unavailable to the liquid molecules; and when objects approach to the extent that these volumes overlap, the molecules have more volume to explore [2, 3]. Thus objects are more likely to be near each other, as if they attract. This entropic force is called “depletion”.

Since the seminal papers of Asakura and Oosawa, depletion forces have had far reaching implications from molecular physics [4–8] and biochemistry [9–11], to high energy physics [12–16]. It has even been suggested that gravity [17–20] and the Coulomb force [21] might stem from depletion. So far, depletion forces between plates immersed in rods [22, 23] or spherocylinders [24], forces between colloids [25], semiflexible chains [26], spherocylinders [27], and ellipsoids [28, 29] immersed in colloids, and forces between colloids immersed in polymer [30] have been established. Forces mediated by mixtures of two types of particles have also been studied [31].

While depletion forces always originate from disordered arrangements of a solvent, the objects experiencing the force themselves have always been chosen by authors to be orderly geometric shapes, such as planes, cylinders and spheres. In this work, we study for the first time, the depletion forces between two disordered objects. We analytically derive the depletion force between two linear disordered macromolecules.

Specifically, we first solve for the depleted liquid density profile surrounding a disordered granular chain, then calculate the free energy and associated entropic force between two such chains, and lastly, we verify both results with realistic molecular dynamics simulations.

A granular chain is a linear arrangement of hard spheres [32], similar to a necklace. Their equilibrium [33–35] transport [36–42] and diffusion [43] properties provide insights into the physics of polymers [44] and biological macromolecules [45, 46]. Decoration and tapering [47, 48], interfaces [49, 50], impurities [51–53], disorder and quasiperiodicity [51–54] are also of interest.

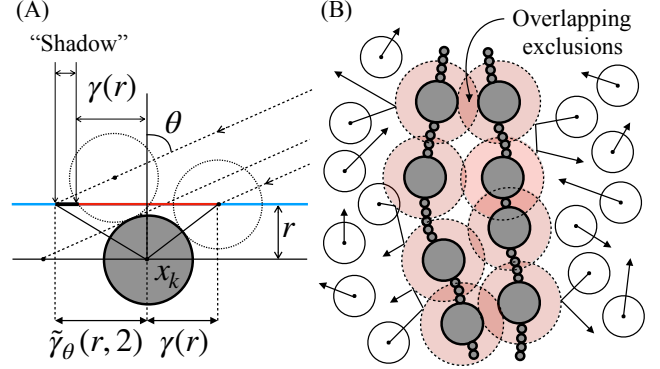


FIG. 1. Notation and problem setup. (A): For a given distance r from the central axis of the chain, if a launched disk is to make it to a point where it is at a height r above the axis, its path must not lead it through excluded regions. A region $\gamma(r)$ to the right, and $\tilde{\gamma}_\theta(r)$ to the left of each disk is excluded. The fact that $\tilde{\gamma}_\theta$ can differ from γ for large enough angles is due to the “shadow” of exclusion which can occur, where for a disk to be able to hit the line at a height r , it must clear the top of the disk at x_k . **(B):** Our random polymers are modeled as chains of spheres of total length L made out of two types of monomers, with radii $r_p > r_c$. Spring forces bonds keep adjacent monomers together, and an angle bonded force penalizes the chain for bending too much. The primary monomers, r_p , interact with hard sphere forces, while the chain monomers, r_c do not interact, serving only as sites for the harmonic and angle bonded forces. Entropic forces arise since it is favorable for the excluded regions of the large monomers to overlap with one another.

LIQUID DENSITY PROFILE NEAR A DISORDERED CHAIN

Consider a line of length L with N non-overlapping, but otherwise randomly-placed spheres of radius R .

We define the stopping function, $R_1\gamma(r)$ as the contact position of a sphere of radius R_2 launched towards another sphere of radius R_1 , with impact parameter rR_1 .

$$\gamma(r, \kappa) = \begin{cases} \kappa \sqrt{1 - (r/\kappa)^2} & r \leq \kappa \\ 0 & r > \kappa \end{cases}. \quad (1)$$

where $\kappa \equiv 1 + R_2/R_1$ is the interaction range factor.

For the usual case where $R_1 = R_2$, $\gamma(r) = \gamma(r, 2) = 2\sqrt{1 - r^2/4}$.

Equivalently, since $\gamma(\gamma(r, \kappa), \kappa) = r$ for $r \leq \kappa$, $\gamma(r)$ is the impact parameter necessary for a sphere to stop at a height r . Much of our analysis can be generalized to arbitrary shapes by simply replacing the sphere stopping function with the appropriate stopping function. Throughout, we define all lengths in units of R , so that $\gamma(r)$ and r are dimensionless.

A liquid molecule will rarely find the opportunity to penetrate all the way to the central axis of a chain. Thus, the expected density of liquid must increase as we move away from the central axis of the chain. To estimate this density profile, we will calculate the probability that a molecule incident towards the chain can approach it by a distance r before contact.

Given a configuration of spheres positioned on the x -axis with x coordinates $\{x_0, \dots, x_{N-1}\}$, and a launching angle of θ with respect to the vertical, we will count up the fraction of the interval $[0, L)$ in which the launched sphere could have started such that it will make it to a distance at least r above the line. We will then integrate over all valid configurations of spheres. We will suppress writing the explicit κ dependence of γ and other functions, for brevity. See Fig. 1 for a depiction of the system, as well as a depiction of the polymer system.

The measure of configurations of spheres on a line is equivalent to the configurations of hard lines on a line, known as a Tonks gas [55, 56]. We write it as

$$\Gamma_N = \int D\mathbf{x} \equiv \frac{L}{N} \prod_{k=1}^{N-1} \int_{x_{k-1}+2\sigma}^{L-2\sigma(N-k)} dx_k = \frac{L^N}{N!} (1 - \phi)^{N-1}. \quad (2)$$

Suppose the x coordinate of the launched sphere at the point where its y component would be r is x_p . Each sphere in the chain excludes a distance $\gamma(r)$ to its right, and $\tilde{\gamma}_\theta(r, \kappa)$ to its left, where

$$\tilde{\gamma}_\theta(r, \kappa) = \begin{cases} 0 & r \geq \kappa \\ \gamma(r, \kappa) & \kappa > r \geq r_0 \\ (r_0 - r) \tan \theta + \gamma(r_0, \kappa) & r_0 > r \geq 0 \end{cases} \quad (3)$$

where $r_0 = r_0(\theta) \equiv \kappa \sin \theta$. The case for $\kappa \tan \theta > r$ emerges because of the “shadow” the excluded volume that a sphere casts on the line.

Suppose that $x_p \in [x_k, x_{k+1}]$. Then probability that it is able to approach to a distance r above the line is proportional to the volume (length) of $[x_k, x_{k+1}]$ that is not excluded by γ or $\tilde{\gamma}$

$$Pr(r | x_p \in [x_k, x_{k+1}]) = \frac{\Xi(x_k - x_{k+1} - 2Rg(r))}{x_{k+1} - x_k}$$

where $g(r) \equiv \frac{1}{2}(\gamma(r) + \tilde{\gamma}(r))$, and the clamp function $\Xi(x)$ is $\Xi(x) = x$ for $x > 0$ and $\Xi(x) = 0$ for $x \leq 0$. The clamp

function is necessary, because the excluded areas of γ and $\tilde{\gamma}$ may overlap. Since the particle’s intersection position, x_p will be in $[x_0, x_1]$ or in $[x_1, x_2]$, etc., and the particle is initialized uniformly at random,

$$\begin{aligned} Pr(r | \vec{x}) &= \sum_{k=0}^{N-1} Pr(r | x_p \in [x_k, x_{k+1}]) Pr(x_p \in [x_k, x_{k+1}]) \\ &= \frac{1}{L} \sum_{k=1}^N \Xi(x_k - x_{k-1} - 2Rg(r)) \end{aligned} \quad (4)$$

Therefore, to obtain $p_\phi(r, N) = Pr(r)$ we just need to integrate over all the arrangements of x_k ,

$$p_\phi(r, N) = \frac{1}{\Gamma_N} \int D\mathbf{x} \frac{1}{L} \sum_{k=1}^N \Xi(x_k - x_{k-1} - 2Rg(r)) \quad (5)$$

where the integration measure is the same as (2), and $1/\Gamma_N$ comes from the normalization of the measure, since we are averaging over all valid configurations of spheres.

If $r > 2$, then $p_\phi(r, N) = 1$. If r is large enough that $g(r) \leq 1$, then every Ξ function is non-zero, and the sum in (5) telescopes and can be evaluated easily,

$$\frac{1}{L} \sum_{k=1}^N \Xi(x_k - x_{k-1} - 2\sigma g(r)) = 1 - \phi g(r)$$

which is independent of any of the positions of the spheres on the line. This term then pulls out of the integral, which cancels with the factor of $1/\Gamma_N$, leaving us with

$$p_\phi(r, N, \theta) = 1 - \phi g(r) : g(r) \leq 1. \quad (6)$$

If $g(r) > 1$, integrating (5) is more involved, since the clamp functions can be zero (see Appendix A),

$$\begin{aligned} p_\phi(r, N, \theta, \kappa) &= \dots \\ &\begin{cases} 1 - \phi g(r) & g(r) \leq 1 \\ (1 - \phi) \left(1 - \phi \frac{g(r)-1}{N(1-\phi)}\right)^N & 1 < g(r) \leq \left(\frac{N}{\phi} - N\right) + 1 \\ 0 & N\left(\frac{1}{\phi} - 1\right) + 1 < g(r) \end{cases} \end{aligned} \quad (7)$$

In the thermodynamic limit $N, L \rightarrow \infty$, $N/L = \phi/(2R)$,

$$p_\phi(r, \theta, \kappa) = \begin{cases} 1 - \phi g(r) & g(r) \leq 1 \\ (1 - \phi) \exp\left[\frac{\phi(1-g(r))}{1-\phi}\right] & g(r) > 1 \end{cases} \quad (8)$$

This is our first main result. Remember, $g(r)$ is actually a function of κ , θ , and r .

Discussion. The approach probability (7) can be viewed in several ways. The first is of course, that $p(r)$ is the probability that a sphere launched at an angle at a disordered chain will approach it by r before colliding. Equivalently, $p(r/\cos \theta)$ is the probability that a sphere launched at an angle towards a *straight* chain will be able to approach it by r . A second way of looking at (7) is

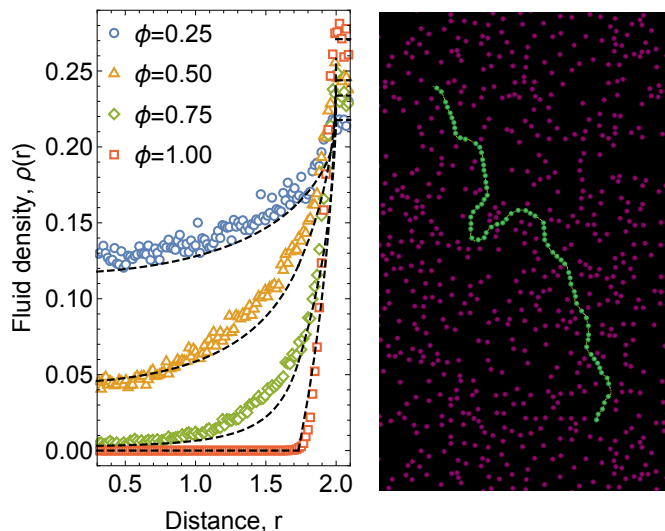


FIG. 2. **Density profile of hard sphere gas and polymer.** **Left:** The density profile of a hard sphere fluid as a function of distance from the closest sphere in a polymer (either large or small). Four different polymer densities are plotted. The fit is of the form $\rho(r) = k \cdot p_\phi(r)$, where k is found by requiring the value of $\rho(r)$ to be the average value of the fit for the sampled points ≥ 2.0 . **Right:** A snapshot of part of the system containing a polymer at an instant in time. The gas particles are magenta, the primary monomers are green, and the chain monomers are yellow and very small.

that its limiting case is the probability that there is a gap of size $g(r)R$ in a Tonks gas. Indeed, the probability that there is a gap of size x at a generic point in a Tonks gas in the thermodynamic limit is [56–58]

$$P(x) = (1 - \phi) \exp[-\phi(2x - 1)/(1 - \phi)].$$

The third view, which we will use to calculate the entropic force, is that $p_\phi(r) \equiv p_\phi(r, \theta = 0)$ is the expected free volume r away from the chain. Indeed, molecular dynamics simulations confirm that even for polymers that are not straight, but simply have an angle potential that keeps them locally “reasonably straight,” using $k \cdot p_\phi(r)$ is a good approximation of the pair correlation between the particles in the polymer and the hard sphere gas it is dissolved in, see Fig. 2. The one free parameter, k , can be fixed by setting k to be the empirical ρ at $r = 2$.

The approach probability can easily be generalized to give the approach probability in three dimensions. If distance of closest approach of the straight line path of the launched sphere and the line the other spheres lie on is s , then the passing probability $p(r, s)$ is simply (8) with all instances of $\gamma(r, \kappa)$ replaced with $\gamma(r, \kappa) \cdot \gamma(s, \kappa)$. This takes into account that the spheres projected into the plane that splits s in two are disks of radius $\gamma(s, \kappa)R/\kappa$.

A numerical test of the passing probability for straight and angled lines is shown in Fig. 3.

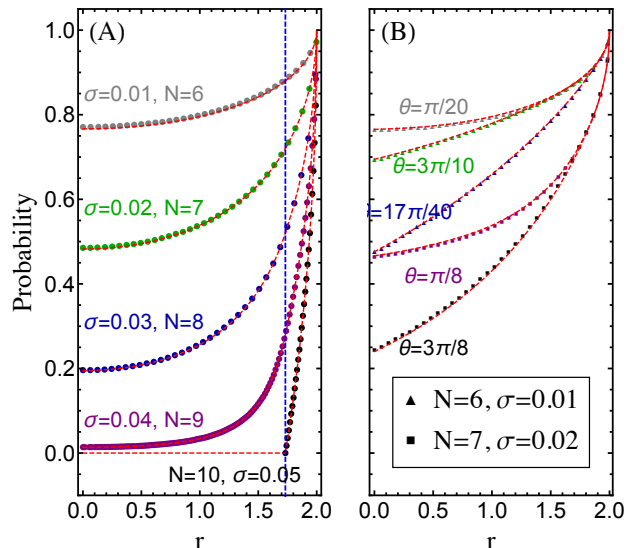


FIG. 3. **Probability of contact of a particle approaching a chain.** Verifying theory (red dashes) with simulations (dots). **(A):** Comparison of simulation and theory for disk launched directly at a line ($\theta = 0$) (7) with $\theta = 0, L = 1$. The vertical blue dashed line represents the point where the piece-wise function (7) transitions at $\gamma = 1$, for $r = \sqrt{3}$. **(B):** Comparing simulations and theory for particles approaching chains at various angles, $\theta \neq 0$.

DEPLETION FORCE BETWEEN DISORDERED CHAINS

Suppose that there are two parallel lines of length L with sphere densities ϕ and φ a distance $x = (2 + h)R$ away from one another. As before, the radius of a sphere is R . Suppose that the lines are in a 2D system of hard spheres, also with radius R , and with number density $\rho = N_s/V$, total volume (area) V , and temperature T . If the lines are closer than $h = 1$, the excluded volumes of the spheres on separate lines can overlap, resulting in an entropic force. The entropic force will depend the arrangement of spheres on each line, which are random variables, but we can calculate the average entropic force between the lines (which becomes exact as the line length $L \rightarrow \infty$) using (8). From here on, by $p_\phi(r)$, we mean $p_\phi(r, 0, 0)$, i.e. $\theta = 0, \kappa = 2$.

If the lines themselves cannot interact ($h > 0$), then the arrangements of spheres on each line is independent. The expression $p_\phi(r)$, (8), tells us the probability that a point a distance r from a line can be occupied by a sphere. Letting rR denote the distance of a point from the left line, $r'R = (2 + h - r)R$ is the distance of that point from the right line. For points at distances $0 < r < h$, a sphere can only be excluded by spheres on the left line, the the probability that a sphere can occupy the volume is $p_\phi(r)$. For points at distances $h < r < 2$, a sphere can be excluded by spheres on either line, so the probability that a sphere can occupy the volume is $p_\phi(r) p_\varphi(h + 2 - r)$.

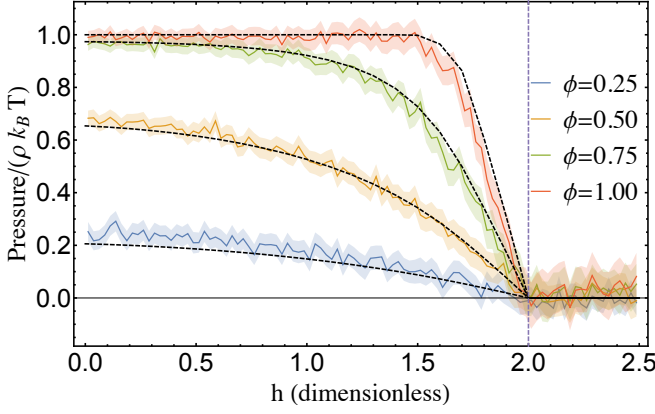


FIG. 4. **Entropic force per unit length between two disordered lines, immersed in a liquid of hard spheres.** Comparing analytical formulas (dashed lines) to molecular dynamics simulations (solid lines). The standard deviation of the mean, $\sigma_\mu = \sigma/\sqrt{N}$, of the simulations are marked with shaded regions representing $2.5\sigma_\mu$. Pressures for systems with lines with density various densities, binned by chain separation, h . The red vertical dashed line marks $h = 2$, beyond which the entropic force vanishes.

Finally, for points at distances $2 < r < 2 + h$, a sphere can only be excluded by the right line, so the probability that a sphere can occupy the volume is $p_\varphi(h + 2 - r)$.

Depletion Force. Each of these expressions involving p 's is the expected free volume per length at points between the lines. From this, we can calculate the free energy of the system, and then the entropic force. The partition function is

$$Z(h) = \frac{V_E(h)^N}{N! \Lambda^{2N}} \quad (9)$$

where $\Lambda = h/\sqrt{2\pi m k_B T}$ is the kinetic part (the h in Λ is Planck's constant), and $V_E(h)$ is the free volume of the system. The expected free volume of the system is

$$V_E(h) = V - v_{\text{out}} - Lh + L\lambda(h). \quad (10)$$

The term v_{out} corresponds to the reduced expected volume to the left of the left chain and right of the right chain, which can also be expressed in terms of p , but does not depend on h , so it will not matter to the entropic force calculation. In the third and fourth term, we subtract the volume between the lines, and add back the expected volume between the lines. From the considerations in the last section, we know that

$$\lambda(h) = \int_0^h p_\phi(r) dr + \int_h^2 p_\phi(r) p_\varphi(r') dr + \int_2^{2+h} p_\varphi(r') dr.$$

where $r' \equiv h + 2 - r$. Then, the total free energy $F = -k_B T \log Z$ is

$$F(h) = F_0 - Nk_B T \log \left[1 - \frac{v_{\text{out}}}{V} - \frac{L}{V} (h - \lambda(h)) \right]$$

where F_0 is independent of h . In the thermodynamic limit $V \rightarrow \infty$, we use $\log(1+x) \simeq x$ to get

$$F(h) \simeq F'_0 - \rho k_B T [h - \lambda(h)] L.$$

Then the force per unit length $\mathcal{P}(h) = -L^{-1} \partial F / \partial h$, is

$$\mathcal{P}(h) = \rho k_B T \left[1 - p_\varphi(h) + \int_h^2 p_\phi(r) \partial_r p_\varphi(h + 2 - r) dr \right] \quad (11)$$

which is our final main result. Note that the expression is the same if ϕ and φ are exchanged (which can be easily seen from integration by parts), and so \mathcal{P} can be written in a symmetric form if that is preferred. Furthermore, \mathcal{P} is always negative, so the entropic force is attractive.

To test our prediction, we ran molecular dynamics simulations [59] for $\phi = \varphi$ measuring the force on disordered lines, and binning this by line separation. The lines were arranged to be rigid, and constrained to only move in the horizontal direction for computational simplicity. The right line was displaced in the y direction to start a distance between 0 and $2R$ above the start of the left line to make sure the measurements were not effected by systematic correlations between the spheres on the two lines, which can occur at high ϕ . At distances greater than $5R = 2.5h$, a harmonic force would activate to keep the lines reasonably close to each other. The results of simulations for different ϕ values can be seen in Fig. 4.

While eq. (11) is exact, it is not practical to evaluate the integral when, say, simulating a large ensemble of chains. For such practical purposes we provide an approximate form for $\phi = \varphi$, obtained using [60],

$$\mathcal{P}(h) = (c_1 + c_2 h^4) \phi^2 - \tanh[(c_3 + h^2) \phi^2] (c_4 + c_5 \tanh[4\phi^4])$$

in units of $\rho k_B T$. Here $c_1 = -0.158$, $c_2 = 0.031$, $c_3 = 3.667$, $c_4 = 0.899$ and $c_5 = 0.236$. This approximates (11) with 0.5% mean error, and 2.5% maximum error.

An analogous calculation can be carried out in three dimensions, an extra integral is needed to compute the free volume for particles not directly between the two lines. The analysis follows exactly the same path, but is more difficult to notate, due to integrals over two dimensional, non-rectangular regions formed by the intersections and complements of circular areas which depend on h . The derivative of the volume may then be computed via the Reynolds transport theorem, the higher dimensional analog of the Leibniz integral rule.

Appendix A

The evaluation (5) when $\tilde{\gamma}_\theta(r) > 1$ is more involved. First, exchange the order of the sum and integrals, then look at each term in the sum,

$$p_\phi(r, N) = \frac{1}{L\Gamma_N} \sum_{j=1}^N T_j(r) \quad (12)$$

$$T_j(r) \equiv \int_{x_0+2\sigma}^{L-2\sigma(N-1)} dx_1 \cdots \int_{x_{j-1}+2\sigma}^{L-2\sigma(N-j)} dx_j \Xi(x_j - x_{j-1} - 2\sigma \tilde{\gamma}_\theta(r)) \int_{x_j+2\sigma}^{L-2\sigma(N-j-1)} dx_{j+1} \cdots \int_{x_{N-2}+2\sigma}^{L-2\sigma} dx_{N-1}. \quad (13)$$

But since our choice of which sphere was 0 is arbitrary, and we are using harmonic boundary conditions (so there is circular symmetry), we must have that $T_j(r) = T_k(r)$ for all pairs j, k . In other words, all the T_j are equal, call this common value $T(r)$. We will evaluate the one that requires the least work, $T(r) = T_1(r)$, since we can integrate all the integrals after the Ξ function inductively.

$$\begin{aligned} T(r) &= \int_{x_0+2\sigma}^{L-2\sigma(N-1)} dx_1 \Xi(x_1 - x_0 - 2\sigma \tilde{\gamma}_\theta(r)) \int_{x_1+2\sigma}^{L-2\sigma(N-2)} dx_2 \cdots \int_{x_{N-2}+2\sigma}^{L-2\sigma} dx_{N-1} \\ &= \int_{x_0+2\sigma}^{L-2\sigma(N-1)} dx_1 \frac{\Xi(x_1 - x_0 - 2\sigma \tilde{\gamma}_\theta(r))}{(N-2)!} \times (L - 2\sigma(N-1) - x_1)^{N-2} \end{aligned} \quad (14)$$

We can deal with the Ξ function by adjusting the bounds of integration. Making the necessary adjustments,

$$T(r) = \frac{1}{(N-2)!} \int_{x_0+2\sigma \tilde{\gamma}_\theta(r)}^{L-2\sigma(N-1)} dx_1 (x_1 - x_0 - 2\sigma \tilde{\gamma}_\theta(r)) (L - 2\sigma(N-1) - x_1)^{N-2} \quad (15)$$

if $\tilde{\gamma}_\theta(r) - 1 < N(1/\phi - 1)$, and is 0 otherwise.

It is safe to exchange the lower bound of integration in (13), $x_0 + 2\sigma$, with $x_0 + 2\sigma \tilde{\gamma}_\theta(r)$ since we are treating the case that $\tilde{\gamma}_\theta(r) > 1$. The second case comes from the fact that $\tilde{\gamma}_\theta(r) - 1 \geq N(1/\phi - 1)$ means that the lower bound of integration would have to be above the upper bound. The T integral can be performed as follows, call $\alpha \equiv 2\sigma \gamma(r)$ and $\beta \equiv L - 2\sigma(N-1)$. Then

$$\begin{aligned} T(r) &= \int_{\alpha}^{\beta} dx (x - \alpha)(\beta - x)^{N-2} \\ &= \int_0^{\beta-\alpha} du (\beta - \alpha - u) u^{N-2} \\ &= \frac{(\beta - \alpha)^{N-1}}{N(N-1)} \\ &= \frac{L^N}{N(N-1)} \left(1 - \phi \left[1 + \frac{\gamma(r) - 1}{N} \right] \right)^N \end{aligned}$$

In to go from the first to the second line, we made the substitution $u = \beta - x$. The integral is then just two polynomial integrals which can be performed with ease.

$$T(r) = \frac{L^N}{N!} \left(1 - \phi \left[1 + \frac{\tilde{\gamma}_\theta(r) - 1}{N} \right] \right)^N \quad (16)$$

if $\tilde{\gamma}_\theta(r) - 1 < N(1/\phi - 1)$, and is zero otherwise. This can be put into (12) and gives us our approach probability for $\tilde{\gamma} > 1$, and can be combined with (6) to yield our complete expression for approach probability.

Appendix B

Here, we give some details about the approach probability for a line, without harmonic boundary conditions. In the thermodynamic limit, the probability is (8), but for finite N, L , there are corrections of order $\mathcal{O}(1/N)$, and the problem is more complicated. For simplicity, we assume that the spheres are of equal size (so $\kappa = 2$), and that $\theta = 0$.

Let $\Gamma_{N,\sigma,L}^{(l)}$ be the measure of configurations of N spheres of radius σ on a line of length L such that no sphere extends “beyond” the line - that is the centers of the spheres must fall in the range $[\sigma, L - \sigma]$. We suppose that the line is along the x axis, from 0 to L . Using the same methods used to solve the analogous problem with harmonic boundary conditions, we get $\Gamma^{(l)} = \frac{L^N}{N!} (1 - \phi)^N$.

A sphere launched at the line can hit the line of spheres if it has x coordinate in the range $[-\sigma, L + \sigma]$, so we consider our launched spheres to be chosen uniformly at random from this range. A sphere with x coordinate less than x_1 can only interact with the first sphere, likewise, a sphere with x coordinate greater than x_N can only interact with the last sphere.

$$\begin{aligned}
p_\phi^{(l)}(r, N) &= \frac{1}{(L + 2\sigma)\Gamma_N^{(l)}} \left(L(r) + \sum_{j=2}^N S_j(r) + R(r) \right) \\
S_j(r) &\equiv \int \mathcal{D}x \, \Xi(x_j - x_{j-1} - 2\sigma \gamma(r)) \\
L(r) &\equiv \int \mathcal{D}x \, (x_1 + 2\sigma - \sigma \gamma(r)) \\
R(r) &\equiv \int \mathcal{D}x \, (L - x_N - \sigma \gamma(r)) \\
\int \mathcal{D}x &\equiv \prod_{k=1}^N \int_{x_{k-1}}^{L-2(N-k+1)\sigma} dx_k \big|_{x_0=-2\sigma}.
\end{aligned}$$

In the case where $\gamma < 1$, the $L(r)$, $R(r)$ integrals can be easily evaluated (they have the same value, by symmetry)

$$L(r) = R(r) = \frac{L^{N+1}}{(N+1)!} (1 - \phi)^N \left[1 + (1 - \gamma/2) \frac{\phi}{N} - \frac{1}{2} \phi \gamma \right] \equiv E(r)$$

and the sums telescopes and so can be easily evaluated,

$$p^{(l)}(r) = \frac{1}{1 + \frac{\phi}{N}} \left(1 - \phi \gamma(r) - \frac{\phi}{N} \right)$$

For the $\gamma > 1$ case, all the S_j are equal, like before, and $L(r) = R(r)$ by symmetry. By adjusting the integration bounds in the integral, just as in (15), we can evaluate $S(r)$.

$$S(r) = \frac{L^{N+1}}{(N+1)!} (1 - \phi)^{N+1} \left(1 - \frac{\phi}{1 - \phi} (1 - \gamma) \frac{1}{N} \right)^N \left[1 - \frac{\phi}{1 - \phi} (\gamma - 1) \frac{1}{N} \left(1 - \left(\frac{\phi}{1 - \phi} \times \frac{\gamma - 1}{1 - \frac{\phi}{1 - \phi} (\gamma - 1) \frac{1}{N}} \times \frac{1}{N} \right)^N \right) \right]$$

Putting all this together, we find that the approach probability for a line without harmonic boundary conditions is

$$p^{(l)}(r) = \begin{cases} \frac{1}{1 + \frac{\phi}{N}} \left(1 - \phi \gamma(r) - \frac{\phi}{N} \right) & \gamma(r) \leq 1 \\ \frac{1}{(L+2\sigma)\Gamma^{(l)}} (2E(r) + (N-1)S(r)) & \gamma(r) > 1 \end{cases}.$$

While this equation is much more complex than its harmonic boundary condition counterpart, they both have the same limiting value in the thermodynamic limit.

-
- [1] C. N. Likos, Physics Reports **348**, 267 (2001).
 - [2] S. Asakura and F. Oosawa, The Journal of Chemical Physics **22**, 1255 (1954).
 - [3] S. Asakura and F. Oosawa, Journal of polymer science **33**, 183 (1958).
 - [4] A. P. Minton, Biopolymers: Original Research on Biomolecules **20**, 2093 (1981).
 - [5] A. Gholami, J. Wilhelm, and E. Frey, Physical Review E **74**, 041803 (2006).
 - [6] M. Mravljak, University of Ljubljana, 3 (2008).
 - [7] M. F. Maghrebi, Y. Kantor, and M. Kardar, EPL (Europhysics Letters) **96**, 66002 (2011).
 - [8] L. Sapir and D. Harries, Current opinion in colloid & interface science **20**, 3 (2015).

- [9] D. Hall and A. P. Minton, *Biochimica et Biophysica Acta (BBA)-Proteins and Proteomics* **1649**, 127 (2003).
- [10] Y. Hanlunmyuang, L. Liu, and P. Sharma, *Journal of the Mechanics and Physics of Solids* **63**, 179 (2014).
- [11] M. Braun, Z. Lansky, F. Hilitski, Z. Dogic, and S. Diez, *BioEssays* **38**, 474 (2016).
- [12] M. Visser, *Journal of High Energy Physics* **2011**, 140 (2011).
- [13] S. Basilakos and J. Sola, *Physical Review D* **90**, 023008 (2014).
- [14] S. Typel, *The European Physical Journal A* **52**, 16 (2016).
- [15] Z.-W. Feng, S.-Z. Yang, H.-L. Li, and X.-T. Zu, *Advances in High Energy Physics* **2016** (2016).
- [16] K. B. Fadafan and S. K. Tabatabaei, *Physical Review D* **94**, 026007 (2016).
- [17] E. Verlinde, *Journal of High Energy Physics* **2011**, 29 (2011).
- [18] A. Plastino and M. Rocca, *Physica A: Statistical Mechanics and its Applications* **505**, 190 (2018).
- [19] A. Plastino, M. Rocca, and G. Ferri, *Physica A: Statistical Mechanics and its Applications* **511**, 139 (2018).
- [20] S. Bhattacharya, P. Charalambous, T. N. Tomaras, and N. Toubas, *The European Physical Journal C* **78**, 627 (2018).
- [21] T. Wang, *Physical Review D* **81**, 104045 (2010).
- [22] Y. Mao, M. Cates, and H. Lekkerkerker, *The Journal of chemical physics* **106**, 3721 (1997).
- [23] Y.-L. Chen and K. S. Schweizer, *The Journal of chemical physics* **117**, 1351 (2002).
- [24] Y. Mao, P. Bladon, H. N. W. Lekkerkerker, and M. E. Cates, *Molecular Physics* **92**, 151 (1997).
- [25] J. C. Crocker, J. A. Matteo, A. D. Dinsmore, and A. G. Yodh, *Physical review letters* **82**, 4352 (1999).
- [26] M. Castelnovo and W. Gelbart, *Macromolecules* **37**, 3510 (2004).
- [27] W. Li and H. Ma, *The European Physical Journal E* **16**, 225 (2005).
- [28] P.-M. König, R. Roth, and S. Dietrich, *Physical Review E* **74**, 041404 (2006).
- [29] H. Miao, Y. Li, and H. Ma, *The Journal of Chemical Physics* **140**, 154904 (2014).
- [30] A. Striolo, C. M. Colina, K. E. Gubbins, N. Elvassore, and L. Lue, *Molecular Simulation* **30**, 437 (2004).
- [31] D. A. Triplett and K. A. Fichthorn, *The Journal of chemical physics* **133**, 144910 (2010).
- [32] C. Chong and P. G. Kevrekidis, *Coherent Structures in Granular Crystals: From Experiment and Modelling to Computation and Mathematical Analysis* (Springer, 2018).
- [33] E. Ben-Naim, Z. Daya, P. Vorobieff, and R. E. Ecke, *Physical review letters* **86**, 1414 (2001).
- [34] K. Safford, Y. Kantor, M. Kardar, and A. Kudrolli, *Physical Review E* **79**, 061304 (2009).
- [35] M. Hastings, Z. Daya, E. Ben-Naim, and R. Ecke, *Physical Review E* **66**, 025102 (2002).
- [36] C. Coste, E. Falcon, and S. Fauve, *Physical review E* **56**, 6104 (1997).
- [37] A. Rosas and K. Lindenberg, *Physical Review E* **69**, 037601 (2004).
- [38] J. Hong, J.-Y. Ji, and H. Kim, *Physical review letters* **82**, 3058 (1999).
- [39] S. Sen, J. Hong, J. Bang, E. Avalos, and R. Doney, *Physics Reports* **462**, 21 (2008).
- [40] J.-G. Cui, T. Yang, and L.-Q. Chen, *Applied Physics Letters* **112**, 181904 (2018).
- [41] P. Gélât, J. Yang, O. Akanji, P. Thomas, D. Hutchins, S. Harput, S. Freear, and N. Saffari, *The Journal of the Acoustical Society of America* **141**, 4240 (2017).
- [42] E. Kim, A. J. Martínez, S. E. Phenisee, P. Kevrekidis, M. A. Porter, and J. Yang, *Nature communications* **9**, 640 (2018).
- [43] F. S. Taheri, H. Fazli, M. Doi, and M. Habibi, *Soft Matter* (2018).
- [44] Z. Ding, J. Aklonis, and R. Salovey, *Journal of Polymer Science Part B: Polymer Physics* **29**, 1035 (1991).
- [45] G. Arya, Q. Zhang, and T. Schlick, *Biophysical journal* **91**, 133 (2006).
- [46] H. Sedgwick, K. Kroy, A. Salonen, M. Robertson, S. Egelhaaf, and W. Poon, *The European Physical Journal E* **16**, 77 (2005).
- [47] R. Doney and S. Sen, *Physical review letters* **97**, 155502 (2006).
- [48] U. Harbola, A. Rosas, A. H. Romero, M. Esposito, and K. Lindenberg, *Physical Review E* **80**, 051302 (2009).
- [49] V. Nesterenko, C. Daraio, E. Herbold, and S. Jin, *Physical review letters* **95**, 158702 (2005).
- [50] C. Daraio, V. Nesterenko, E. Herbold, and S. Jin, *Physical Review Letters* **96**, 058002 (2006).
- [51] A. Sokolow and S. Sen, *Annals of Physics* **322**, 2104 (2007).
- [52] A.-L. Chen and Y.-S. Wang, *Physica B: Condensed Matter* **392**, 369 (2007).
- [53] F. Fraternali, M. A. Porter, and C. Daraio, *Mechanics of Advanced Materials and Structures* **17**, 1 (2009).
- [54] A. J. Martínez, P. G. Kevrekidis, and M. A. Porter, *Physical Review E* **93**, 022902 (2016).
- [55] L. Tonks, *Physical Review* **50**, 955 (1936).
- [56] P. V. Giaquinta, *Entropy* **10**, 248 (2008).
- [57] S. Torquato, B. Lu, and J. Rubinstein, *Physical Review A* **41**, 2059 (1990).
- [58] Z. Elkoshi, H. Reiss, and A. D. Hammerich, *Journal of statistical physics* **41**, 685 (1985).
- [59] Using the GFlow molecular dynamics package, <https://github.com/nrupprecht/GFlow>.
- [60] L. H. Schmidt M., “Eureqa (version 0.98 beta),” (2014).